Hydrogen-Deuterium Exchange Effects on β-Endorphin Release from AtT20 Murine Pituitary Tumor Cells

Masayuki Ikeda,*† Shigeru Suzuki,‡ Masahiro Kishio,‡ Moritoshi Hirono,* Takashi Sugiyama,‡ Junko Matsuura,‡ Teppei Suzuki,§ Takayuki Sota,§ Charles N. Allen,¶ Shiro Konishi,‖ and Tohru Yoshioka*‡

*Advanced Research Institute for Science and Engineering, Waseda University, 3-4-1 Okubo Shinjuku-ku, Tokyo 169-8555, Japan; †Department of Molecular Behavioral Biology, Osaka Bioscience Institute, 6-2-4 Furuedai, Suita, Osaka 565-0874, Japan; ‡Department of Molecular Neurobiology, School of Human Sciences, Waseda University, 2-579-15 Mikajima, Tokorozawa, Saitama 359-1192, Japan; §School of Science and Engineering, Waseda University, 3-4-1 Okubo Shinjuku-ku, Tokyo 169-8555, Japan; ¶Center for Research on Occupational and Environmental Toxicology, Oregon Health and Science University, Portland, Oregon 97201-3098, USA; and ‖Mitsubishi Kagaku Institute of Life Sciences, and Core Research for Evolutional Science and Technology (CREST), Japan Science and Technology Agency (JST), 11 Minamiooya, Machida-shi, Tokyo 194-8511, Japan

ABSTRACT Abundant evidences demonstrate that deuterium oxide (D_2O) modulates various secretory activities, but specific mechanisms remain unclear. Using AtT20 cells, we examined effects of D_2O on physiological processes underlying β-endorphin release. Immunofluorescent confocal microscopy demonstrated that 90% D_2O buffer increased the amount of actin filament in cell somas and decreased it in cell processes, whereas β-tubulin was not affected. Ca^{2+} imaging demonstrated that high-K^+-induced Ca^{2+} influx was not affected during D_2O treatment, but was completely inhibited upon D_2O washout. The H_2O/D_2O replacement in internal solutions of patch electrodes reduced Ca^{2+} currents evoked by depolarizing voltage steps, whereas additional extracellular H_2O/D_2O replacement recovered the currents, suggesting that D_2O gradient across plasma membrane is critical for Ca^{2+} channel kinetics. Radioimmunoassay of high-K^+-induced β-endorphin release demonstrated an increase during D_2O treatment and a decrease upon D_2O washout. These results demonstrate that the H_2O-to-D_2O-induced increase in β-endorphin release corresponded with the redistribution of actin, and the D_2O-to-H_2O-induced decrease in β-endorphin release corresponded with the inhibition of voltage-sensitive Ca^{2+} channels. The computer modeling suggests that the differences in the zero-point vibrational energy between protonated and deuterated amino acids produce an asymmetric distribution of these amino acids upon D_2O washout and this causes the dysfunction of Ca^{2+} channels.

INTRODUCTION

Deuterium, a heavy and stable isotope of hydrogen, binds to oxygen to form deuterium oxide (D_2O), commonly known as heavy water. D_2O exists in the environment at 1/6700 of H_2O, and is expected to have some biological effects, deleterious and otherwise, on whole animals, animal cells, microorganisms, and macromolecules (Kushner et al., 1999), but many of these effects remain uncharacterized.

The effects of D_2O on cellular secretion have been extensively studied in various cell types without any consensus on the underlying mechanisms. For example, D_2O significantly reduces insulin release from pancreatic islets (Malaisse-Lagae et al., 1971; Freinkel et al., 1976; Montague et al., 1976; Hill and Rhoten, 1983), amylase release from pancreatic fragments (Calderon et al., 1980), and gastrin release from antral mucosal fragments (Harty et al., 1983). D_2O has been shown to modulate the amount and arrangement of microtubules (Malaisse-Lagae et al., 1971; Houston et al., 1974; Itoh and Sato, 1984) and secretory granules are transported from the basal to the apical cytoplasm via microtubules (Lacy et al., 1968; Malaisse et al., 1975; Sasaki and Tashiro, 1976), thus the D_2O-induced decrease in secretion has been ascribed to the stabilization of microtubules (Malaisse-Lagae et al., 1971; Montague et al., 1976; Hill and Rhoten, 1983). The mechanism underlying the effect of D_2O may not be this simplistic, however, because it has been shown that D_2O increases serotonin release from blood platelets (Bennett et al., 1979) and spleen cells (Sulowska and Wyczolkowska, 1991) and histamine release from mast cells (Fewtrell and Metzger, 1980; Maeyama et al., 1986) and basophilic leukemia cells (Urata et al., 1989).

Theoretically, D_2O has at least two independent physiological effects: i), an isotope exchange (hydrogen to deuterium) effect on functional proteins, and ii), a solvent isotope effect, meaning that the mobility of monovalent cations is reduced by ~20%, whereas the dielectric constant is not changed in D_2O buffer (Bass and Moore, 1973). The computer simulation studies on the isotope exchange effect using the density functional theory demonstrated that with H_2O to D_2O exchange, the state of functional proteins changes quickly, but with D_2O to H_2O exchange, the state of proteins recovers very slowly, due to the stability of deuterated amino acids (Table 1). On the other hand, reported electrophysiological properties (membrane potential and channel conductances), which are under the influence of a solvent isotope effect, change reversibly and rapidly with the change from H_2O to D_2O and back again

Submitted December 5, 2002, and accepted for publication September 10, 2003.

Address reprint requests to Tohru Yoshioka, PhD, Tel.: +81-3-5286-2761; Fax: +81-3-3205-6419; E-mail: yoshioka@human.waseda.ac.jp.

Tohru Yoshioka's present address is Dept. of Molecular Neurobiology, School of Science and Engineering, Shillman Hall, Room 601, Waseda University, 169-0072 Japan.

0006-3495/04/01/565/11 $2.00

TABLE 1 Electronic (self-consistent field) energy (Hartree), ZPVE (kcal/mol), and ΔZPVE (kcal/mol) of hydrophilic amino acids

	Electronic energy*	ZPVE†		Degrees of isotopic substitutions	ΔZPVE
		Nondeuterated	Deuterated		
Asn	−492.45636	85.52056	83.40989	1	−2.11
			81.25598	2	−4.26
Gln	−531.77310	103.27266	101.22502	1	−2.05
			99.11591	2	−4.16
Ser	−398.96310	71.10529	69.04891	1	−2.06
Thr	−438.28159	88.71962	86.64785	1	−2.07
Tyr	−630.03202	121.80236	119.68360	1	−2.12
Lys‡	−497.30465	142.14074	139.92714	1	−2.21
Arg‡	−606.96343	147.84039	145.74911	1	−2.09
His‡	−549.18674	109.78890	107.71983	1	−2.07
			105.51926	2	−4.28

Acidic amino acids were not calculated because they have no replaceable OH- or NH-bonds in their side chains.
*Calculated at B3LYP/6-31G(d,p) level of theory.
†No scaling factor for ZPVE was used.
‡Calculated from the ionized form.

(Schauf and Bullock, 1979; Schauf and Chuman, 1986; Andjus et al., 1994). Therefore, isotope exchange effects and solvent isotope effects are possibly distinguishable as temporal pattern of D_2O actions. However, D_2O actions on physiological processes such as exocytosis have not been analyzed from this biophysical point of view.

Murine anterior pituitary corticotroph tumor (AtT20) cells are a good model cell-line for the hypothalamo pituitary adrenal axis because they continue to secrete adrenocorticotropic hormone and β-endorphin (Richardson and Schonbrunn, 1981; Richardson, 1983; Westendorf and Schonbrunn, 1985; Schetcterson and McKnight, 1991) and the secretory granules move anterogradely along microtubules (Tooze and Burke, 1987). Therefore, we examined the effects of D_2O on cytoskeletal components that may be closely linked to secretion from AtT20 cells. Because secretion from AtT20 cells depends on the intracellular Ca^{2+} concentration and Ca^{2+} dynamics are regulated largely by voltage-sensitive Ca^{2+} channels (VSCCs) in AtT20 cells (Richardson and Schonbrunn, 1981; Richardson, 1983), we used fura-2-AM-based intracellular Ca^{2+} imaging and whole-cell patch-clamp experiments to analyze the effects of D_2O on VSCCs.

With special cautions for the temporal coordinates of D_2O actions, we found biphasic and bidirectional effects of D_2O on high-K^+-induced β-endorphin secretions in AtT20 cells. The initial increase of secretion corresponds to the immediate redistribution of actin filaments, whereas the delayed inhibition of secretion corresponds to dysfunction of VSCCs upon D_2O washout.

MATERIALS AND METHODS

Cell cultures

AtT20 cells (clone D16V) were cultured at 37°C in Dulbecco's modified eagle medium supplemented with 10% fetal bovine serum in a humidified atmosphere of 95% air and 5% CO_2. For Ca^{2+} imaging and electrophysiological experiments, cells were plated onto 35-mm glass-bottom petri dishes or 12-mm glass cover slips at a density of $\sim 5 \times 10^4$ cells. The culture medium was exchanged every other day and on the day before the experiments.

Immunofluorescent confocal imaging

To observe the effects of D_2O on the cytoskeleton, AtT20 cells were incubated in H_2O-based buffered salt solution (BSS) consisting of (mM) 128 NaCl, 5 KCl, 2.7 $CaCl_2$, 1.2 $MgCl_2$, 1 Na_2HPO_4, 10 glucose, and 10 HEPES/NaOH (pH 7.3) for 20 min, and the H_2O BSS was replaced with 90% D_2O BSS for 5 or 15 min. AtT20 cells were then fixed in 4% phosphate-buffered paraformaldehyde for 15 min and washed three times with phosphate-buffered saline (PBS) consisting of (mM) 137 NaCl, 2.7 KCl, 1.5 KH_2PO_4, and 8.1 Na_2HPO_4 (pH 7.4). The fixed sample was then dipped in acetone for 3 min and dried to facilitate staining of F-actin with rhodamine phalloidin (Molecular Probes, Eugene, OR). The dried sample was incubated for 2 h at room temperature (24–26°C) with monoclonal antibodies against β-tubulin (1:100, ICN Biomedicals, Aurora, OH) and neurofilament-M (1:100, Chemicon International, Temecula, CA) dissolved in PBS supplemented with 1% bovine serum albumin (BSA), 0.1% Triton-X, and 0.05% sodium azide. The sample was rinsed three times with PBS and incubated for 1 h at room temperature with fluorescein isothiocyanate-conjugated goat anti-mouse IgG (ICN Biomedicals, 1:200) and rhodamine phalloidin (1:200) dissolved in the bovine serum albumin-supplemented PBS. After washing out the secondary antibody with PBS, the sample was mounted with glycerol. A confocal imaging system (μ-Radiance, Bio-Rad, Hercules, CA) attached to a fluorescence microscope (AxioPlan2, Carl Zeiss, Oberkochen, Germany) was used with an argon/krypton laser and a 40× objective lens (Plan-Neofluar 40×/0.75, Carl Zeiss). The digital image was processed using Photoshop (Adobe) software. All staining experiments were repeated at least three times.

Ca^{2+} imaging

The culture medium was gently rinsed from dishes using BSS. The cells were then incubated in BSS supplemented with 5 μM fura-2 AM (Molecular Probes) for 30 min in a CO_2 incubator. Before photometry, the cells were rinsed again with BSS, incubated at 37°C for 15 min, and then continuously perfused with BSS at 30°C at a flow rate of 3 ml/min. Fluorescence images were produced by alternating 340- and 380-nm ultraviolet pulses (143-ms duration) and the resulting pairs of images were projected onto a cooled CCD camera (C4880, Hamamatsu Photonics, Hamamatsu, Japan) at 3–6-s intervals. A cocktail of 10 μM nifedipine (Sigma, St. Louis, MO) and 100 nM ω-conotoxin MVIIC (Alomone Labs, Jerusalem, Israel) was used to block VSCCs, because these VSCC blockers at these concentrations inhibit most VSCC subtypes in AtT20 cells (Loechner et al., 1996). Tetrodotoxin (TTX; Alomone Labs) was applied at a concentration of 1 μM to estimate possible involvement of Na^+ channels in the Ca^{2+} oscillations. The frequency of the Ca^{2+} oscillations was estimated by the number of peaks within 180-s blocks recorded during the control and TTX treatment periods. All drugs were bath-applied with the perfusate. Further details of the Ca^{2+} imaging technique have been described previously (Ikeda et al., 2001; Nelson et al., 2001).

Electrophysiology

Recordings were performed at 3–4 days after plating by placing a cover slip fragment into a recording chamber located on the stage of an upright microscope equipped with phase-contrast optics. The chamber was perfused at ~1 ml/min with BSS. Microelectrodes, pulled in two stages (Narishige puller, Narishige, Tokyo, Japan) from thin-walled borosilicate glass (World Precision Instruments, Sarasota, FL), had resistances of 5–7 MΩ when filled with a (intracellular) solution, at pH 7.3 and 310 mOsm, consisting of (mM)

Cs methanesulfonate 87, CsCl 20, CsOH 25, $CaCl_2$ 1, HEPES 10, EGTA 10, ATP 3, and GTP 0.3. For the recording of resting membrane potential of AtT20 cells, the current clamp mode of the whole-cell patch clamp method was used with EPC-8 patch amplifier (HEKA, Lambrecht/Pfalz, Germany). Membrane potential responses were filtered at 3 kHz and acquired using pCLAMP7 software (Axon Instruments, Foster City, CA). For the recording of K^+ currents, the cells were held at −60 mV using the whole-cell configuration of the patch-clamp technique and the membrane voltage stepped to +50 mV once every 30 s. To activate voltage-gated Na^+ currents the cells were voltage clamped at −83 mV and depolarizing steps (10-mV steps, 30 ms in duration) applied once each 4 s. For the recordings of Ba^{2+} currents, Ca^{2+}-free BSS containing 10 mM $BaCl_2$ and 0.5 μM TTX was used as the external solution and 3 μM QX-314 was added to the internal solution. For the recordings of Ca^{2+} currents, internal solutions consisting of (mM) CsCl 120, $MgCl_2$ 3, HEPES 10, EGTA 10, ATP 3, GTP 0.4 and creatine phosphate 14, and external solutions consisting of (mM) TEA-Cl 142, $CaCl_2$ 2.5, MgCl2 1, HEPES 15, and glucose 9.9 were used. To observe intracellular hydrogen/deuterium exchange effects, Ca^{2+} current recordings were initiated with the internal solution of 90% D_2O, and thereafter the external solution was replaced to 90% D_2O-BSS by the bath perfusion. Voltage-gated Ca^{2+} currents were activated from a holding potential of −80 mV with depolarizing pulses (10-mV steps, 50 ms) applied once each 8 s. These currents were recorded using an Axopatch 1C (Axon Instruments), filtered at 2 kHz (−3 dB) with an eight-pole Bessel filter and digitized at 10 kHz on-line using an ITC16 A/D interface (Instrutech, Port Washington, NY) and Pulse software (HEKA). The cell capacitance and series resistance (15–30 MΩ, 80%) were compensated. All records were corrected for a liquid junction potential of −13 mV. Further details of the recording methods have been described previously (Suzuki et al., 1997a,b; Hirono et al., 1999).

Radioimmunoassay for β-endorphin release

AtT20 cells were seeded onto a 100-mm dish (1×10^6 cells/dish) and cultured at 37°C for 24 h in the growth medium. After washing out the growth medium with BSS, the cells were incubated in 4 ml H_2O BSS, D_2O BSS, 30 mM K^+ H_2O BSS, and/or 30 mM K^+ D_2O BSS at room temperature. β-Endorphin concentrations in H_2O BSS (3 min) or in 90% D_2O BSS (3 min) were assayed as undepolarized controls. Three groups were depolarized with high-K^+ concentration and treated with D_2O. The first group (H_2O) was stimulated with 30 mM K^+ H_2O BSS (3 min) without any D_2O treatment. The second group (D_2O) was stimulated with 30 mM K^+/90% D_2O BSS for 3 min. The third group (D_2O wash out) was treated with 90% D_2O BSS for 3 min and then depolarized with 30 mM K^+ H_2O BSS for 3 min during D_2O wash out.

Radioimmunoassays of β-endorphin in these samples were then performed by researchers fully blind to the sample conditions. The antiserum was prepared in a rabbit by several biweekly injections of β-endorphin emulsified in complete Freund's adjuvant. The β-endorphin was labeled using the chloramines-T method and assayed as described previously (Furui et al., 1984). Briefly, the incubation buffer was mixed with 100 mg/ml silicic acid and vortexed vigorously for 5 min. After centrifugation at 3000 rpm at 4°C for 5 min, the pellet was rinsed twice with an equal volume of ice-cold distilled water. The pellet was then extracted with 80% acetone in 0.1 N HCl via vigorous mixing for 5 min and centrifuged at 3000 rpm for 5 min. The supernatant was decanted and evaporated under a flow of nitrogen. The extract was dissolved in 0.2 ml of assay standard buffer (0.1 M phosphate buffer, pH 7.5, containing 0.5% bovine serum albumin and 500 U/ml aprotinin). Standard and samples were each brought to a total volume of 0.25 ml with the addition of standard buffer to achieve the appropriate dilution of antiserum. After incubation for 72 h at 4°C, ^{125}I-labeled β-endorphin was added and the mixture was incubated for 24 h at 4°C. The ^{125}I-β-endorphin was precipitated by the addition of 0.1 ml 0.1% rabbit gamma globulin, 0.5 ml 25% polyethylene glycol, and 0.1 ml standard buffer, and then centrifuged at 3000 rpm for 5 min. The radioactivity of the pellets was used as a quantitative estimation of the net β-endorphin concentrations.

The concentration of β-endorphin measured from each sample (4 ml) after 14–16 h was used to normalize experimental variations among flasks. One measurement from the H_2O group ($n = 6$) and one from the D_2O-pretreated group ($n = 6$) were rejected according to Smirnoff's normality test (5% confidence). Duncan's multiple range test after a one way analysis of variance (ANOVA) was used for the comparison among the groups. A Student's *t*-test was used for statistical comparison unless otherwise noted.

Quantum chemical method

Ab initio calculations were carried out based on the Kohn-Sham density function theory (Kohn and Sham, 1965) using the Becke3-Lee-Yang-Parr (B3LYP) function (Becke, 1993; Lee et al., 1988) and the 6-31G(d,p) basis set. Among available functions, the B3LYP function has been widely used in density-function-theory-based calculations and proven to yield very good descriptions of the vibration frequencies of small organic molecules. Harmonic vibration frequencies were calculated via analytic second derivatives of the energy with respect to the nuclear coordinates. We calculated the zero-point vibration energy of specific amino acids and water molecules, and evaluated the changes in the zero-point vibration energy that accompany the substitution of hydrogen atoms with deuterium atoms. No scaling factor for the zero-point vibration energy was used. All calculations were carried out using Gaussian 98 software (Frisch et al., 1998) on an AlphaSationXP1000 (Compaq Computer K.K., Tokyo, Japan) workstation.

RESULTS

Effects of D_2O on the cytoskeleton

To investigate the effects of D_2O on the cytoskeleton, we examined rhodamine phalloidin labeling of actin filaments and immunostaining of β-tubulin (Fig. 1). Actin filaments were observed as filamentous structures that were found to be more highly concentrated in the cell processes than in cell somas (Fig. 1, *A* and *B*, *a*). Treatment with 90% D_2O BSS for 5 min immediately increased the amount of actin filaments in the cell somas and eliminated its filamentous structure (Fig. 1 *A*). The relative amount of actin filaments in the cell processes was decreased with D_2O treatment (Fig. 1 *B*, *b*). Longer treatment with 90% D_2O BSS (15 min) resulted in an increase in the actin filaments in the cell processes again, however, the filamentous structure was still lacking (Fig. 1 *A*). After D_2O washout, the actin filaments were equally distributed in the cell processes and cell somas (Fig. 1 *B*, *c*). After D_2O washout, the filamentous structure of the actin filaments recovered, but the shape of the filaments in the cell processes was similar to that of varicose filaments (Fig. 1, *A* and *B*, *c*). The original shape of the actin filaments did not recover by 30 min after D_2O washout. Despite the marked changes in the distribution and structure of actin filaments, the amount, distribution, and structure of β-tubulin (Fig. 1 *A*) or neurofilament-M (data not shown) were not changed by D_2O treatment.

Effects of D_2O on spontaneous action potentials

Whole-cell current-clamp recording showed that treatment with 90% D_2O BSS for 1 min resulted in complete inhibition

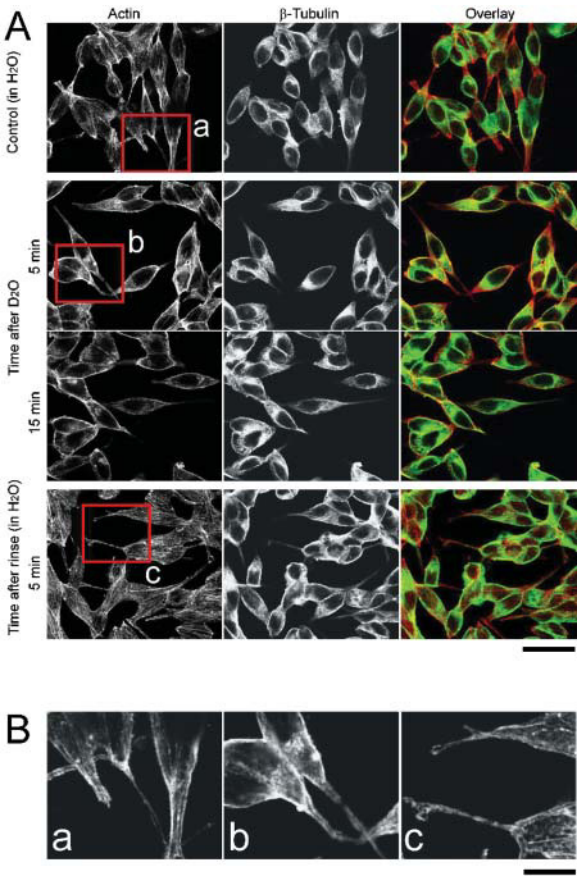

FIGURE 1 (*A*) Effects of 90% D_2O treatment on actin filaments (rhodamine phalloidin labeling, *red*) and β-tubulin (FITC-labeling, *green*) in AtT20 pituitary cells. Short (5 min) treatment with D_2O increased the amount of actin filaments in the cell somas and decreased it in the cell processes. After a 15-min treatment with D_2O, however, the amount of actin filaments in the cell processes increased. After D_2O washout, actin filaments were equally distributed in the cell soma and processes. Short and long treatment with D_2O also eliminated the filamentous structure of actin filaments, which returned immediately (<5 min) after D_2O wash out, but resembled varicose filaments. D_2O treatment had only a small effect on the amount, distribution, or structure of β-tubulin. The typical changes in the distribution of actin filaments (marked as *red frame a–c*) are enlarged in *B*. Bar = 50 μm in *A*, 20 μm in *B*.

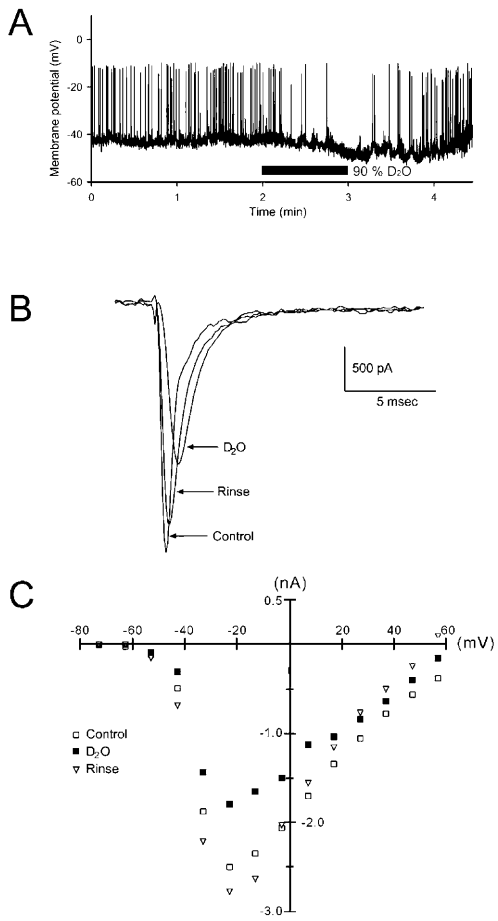

FIGURE 2 Effects of D_2O on spontaneous action potential firing and voltage-gated Na^+ channels. (*A*) Spontaneous action potentials were inhibited in 90% D_2O BSS. This effect was observed in four separate cells. (*B*) Example of voltage-gated Na^+ currents activated before, during, and after application of 90% D_2O. The cell was held at −83 mV and the membrane voltage stepped to −13 mV. Note that the peak of the Na^+ current was delayed compared to the control currents. (*C*) A current-voltage curve (average of three cells) showing the effects of the D_2O solution on the Na^+ current amplitude over a range of depolarizing voltage steps.

of spontaneous action potentials for ~2 min in all cells examined ($n = 4$; Fig. 2 *A*). The mean resting membrane potential during the firing burst (−45.3 ± 1.2 mV, $n = 4$) was slightly hyperpolarized (−54.4 ± 3.4 mV, $n = 4$) immediately after D_2O application.

To observe the direct effects of D_2O on voltage-dependence and conductance of Na^+ channels, we also performed voltage-clamp recordings. Application of a depolarizing voltage steps (30 ms, from a membrane holding potential of −83 mV) to a voltage-clamped AtT20 cell activated voltage-gated Na^+ currents (Fig. 2 *B*). These currents were completely blocked by with 1 μM TTX ($n = 3$; data not shown), proving that they are voltage-gated Na^+ currents. Perfusion with 90% D_2O solution (1–2 min) reduced the peak amplitude of the Na^+ currents by a mean of 76.2 ± 4.8% (Fig. 2 *C*; $n = 3$; $p < 0.01$). During D_2O exposure, Na^+ currents displayed slow rise and slow decay kinetics (Fig. 2 *B*). These effects of D_2O were completely reversible after washout of the D_2O solution with the control extracellular solution.

Effects of D_2O on spontaneous Ca^{2+} oscillations

Spontaneous Ca^{2+} oscillations were observed in approximately half the cells examined (389 of 743 cells, number of experiments = 16). The oscillation frequency varied widely (0.1–0.01 Hz). Cells were treated with 90% D_2O BSS for 90 s, and this resulted in a gradual inhibition of spontaneous Ca^{2+} oscillations for 4–6 min (Fig. 3 *A*). Longer treatment with 50% D_2O BSS (3 min; Fig. 3 *A*) or with lower concentrations of D_2O had little effect on the Ca^{2+}

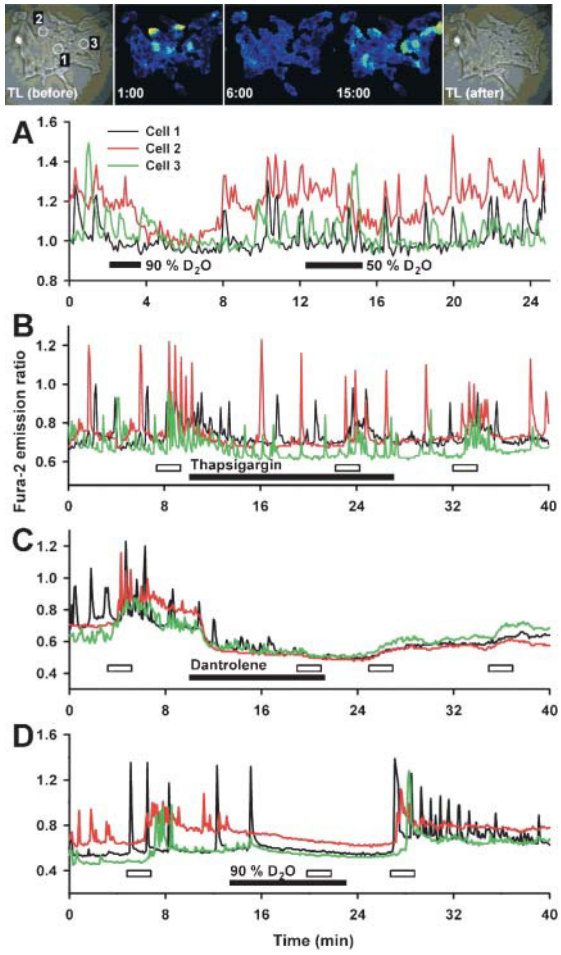

FIGURE 3 Effects of D_2O on spontaneous Ca^{2+} oscillations. (*A*) Treatment with 90% D_2O inhibited spontaneous Ca^{2+} oscillations in AtT20 cells. The time course of intracellular Ca^{2+} concentration in three cells (*Cells 1–3* as *black*, *red*, and *green lines*) that are marked in the transmitted light (*TL*) image on the top. Pseudocolor images on the top showing the changes in the intracellular Ca^{2+} concentration. Increasingly warmer colors indicate higher Ca^{2+} concentrations. Approximately half of the cells in this culture plate exhibited spontaneous Ca^{2+} oscillations, which were inhibited in 90% D_2O BSS. The TL images before and after D_2O treatment revealed that there was little morphological change. Treatment with 50% D_2O BSS partially inhibited spontaneous Ca^{2+} oscillations. (*B–D*) The Ca^{2+} oscillations were repeatedly activated by 120-s exposure to caffeine (2 mM; *white bars*). (*B*) A Ca^{2+}-ATPase inhibitor, thapsigargin (2 μM), inhibited neither spontaneous Ca^{2+} oscillations nor caffeine-induced Ca^{2+} oscillations. (*C*) Dantrolene (30 μM), an inhibitor for the ryanodine receptor, inhibited both spontaneous and caffeine-induced Ca^{2+} oscillations. It was not possible to wash out dantrolene during the recording period. (*D*) The 90% D_2O solution reversibly inhibited spontaneous and caffeine-induced Ca^{2+} oscillations. All experiments were repeated in at least four separate trials.

oscillations. Treatment with TTX (1 μM, for 10 min) had little effect on Ca^{2+} oscillations ($n = 3$), indicating that the Ca^{2+} oscillations were not directly driven by the action potentials.

Since the spontaneous Ca^{2+} oscillations seem to be driven by the release of Ca^{2+} from intracellular Ca^{2+} store, we examined the effect of the ryanodine receptor inhibitor, dantrolene, and the Ca^{2+}-ATPase inhibitor, thapsigargin, on the caffeine (2 mM) activated spontaneous Ca^{2+} oscillations (Fig. 3, *B–D*). It was found that caffeine response was completely blocked by dantrolene (30 μM; number of experiments = 4, Fig. 3 *C*), but not by thapsigargin (2 μM; number of experiments = 4, Fig. 3 *B*). The 90% D_2O for 10 min completely inhibited spontaneous Ca^{2+} oscillations as well as caffeine-activated Ca^{2+} oscillations (number of experiments = 4, Fig. 3 *D*). The effects of D_2O on caffeine-induced Ca^{2+} oscillations were completely reversible after washout of the D_2O solution with the control extracellular solution (Fig. 3 *D*).

Effects of D_2O on high-K^+-induced membrane depolarization and Ca^{2+} influx

AtT20 cells that exhibited no spontaneous action potentials or infrequent Ca^{2+} oscillations were used in the following experiments. Exposure to 30 mM K^+ depolarized the membrane potential from -69.0 ± 3.2 mV to -32.0 ± 3.6 mV ($n = 4$, Fig. 4, *A* and *B*). The resting membrane potential slightly depolarized ($+4.4 \pm 0.6$ mV, $n = 4$) but high-K^+-induced membrane depolarization was not significantly changed with treatment with 90% D_2O BSS ($n = 3$, Fig. 4 *A*). In addition, it was observed that VSCCs were not a primary determinant of the resting membrane potential, because blocking VSCCs with 10 μM nifedipine and 100 nM ω-conotoxin MVIIC failed to reduce the membrane potential ($n = 3$, Fig. 4 *B*). The K^+ currents recorded at holding membrane potential of +50 mV (mean amplitude = 703 $\pm$ 42 pA) was reduced immediately by 90% D_2O BSS perfusion ($-37.5 \pm 6.7\%$, $p < 0.01$ by a paired Student's *t*-test, $n = 4$) and recovered to the control levels 8–9 min after D_2O washout (Fig. 4 *C*).

Exposure to 30 mM K^+ (45 s) produced a reproducible (7-min intervals) and rapid increase in the concentration of intracellular Ca^{2+} (Fig. 5 *A*). This Ca^{2+} response was primarily due to Ca^{2+} influx through VSCCs because VSCC blockers (10 μM nifedipine and 100 nM ω-conotoxin MVIIC) significantly reduced the amplitude of the high-K^+-induced Ca^{2+} response ($-89.5 \pm 9.3\%$, number of experiments = 4, $p < 0.01$ in comparison with first Ca^{2+} response by a paired Student's *t*-test, Fig. 5 *B*). Treatment with 10% D_2O BSS (unpublished data) or 50% D_2O BSS (Fig. 5 *C*) for 3 min had no effect on the high-K^+-induced Ca^{2+} influx. Interestingly, high-K^+-induced Ca^{2+} influx during treatment with 90% D_2O BSS was not changed, whereas the first few high-K^+-induced Ca^{2+} responses during D_2O washout were significantly inhibited ($-99.8 \pm 0.2\%$, number of experiments = 4, $p < 0.01$ in comparison with first Ca^{2+} response by a paired Student's *t*-test, Fig. 5 *D*). This inhibition of high-K^+-induced Ca^{2+} influx was primarily dependent on the time elapsed after D_2O treatment. A 1-min treatment with 90% D_2O BSS was sufficient to inhibit high-K^+-induced

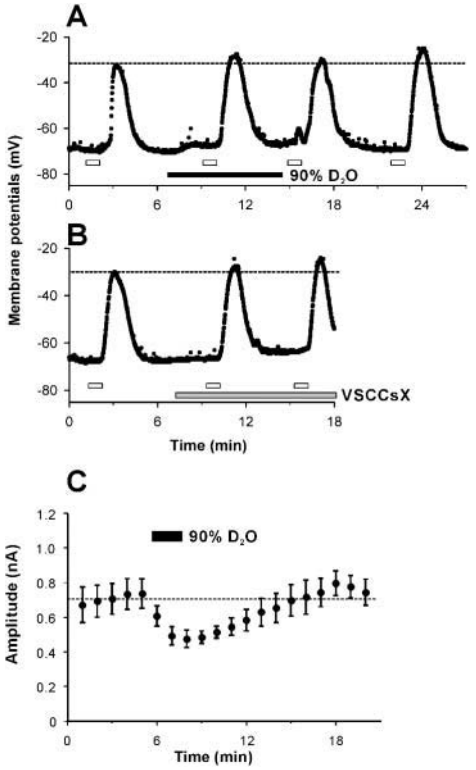

FIGURE 4 Effects of 90% D_2O BSS on high-K^+-induced membrane depolarization and K^+ channel conductance. (*A*) Perfusion of 30 mM K^+ for 45 s (*open bars*) evoked a rapid membrane depolarization. Broken line denotes the peak membrane potential before D_2O treatment. This response was not significantly altered by treatment with 90% D_2O (*black bar*). (*B*) A mixture of voltage-sensitive Ca^{2+} channel blockers (*VSCCsX*, *gray bar*) had no effect on the high-K^+-induced membrane depolarization. Similar responses were observed in four individual cells. (*C*) The K^+ current activated by depolarizing voltage steps was partially reduced by application of 90% D_2O BSS (*black bar*). The cells were held at −60 mV and the membrane voltage stepped to +50 mV to observe K^+ currents. The mean current amplitude ± SE was calculated from four cells. Broken line denotes the mean current amplitude before D_2O treatment.

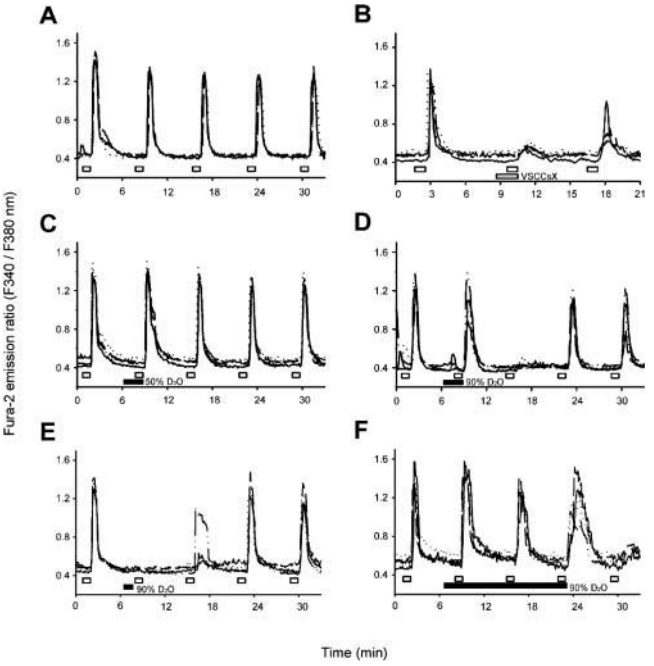

FIGURE 5 The effects of D_2O on the high-K^+-induced Ca^{2+} influx in AtT20 cells. (*A*) 30 mM K^+ (*open bars*) induced a rapid, reproducible (7-min intervals) increase in intracellular Ca^{2+} concentration. (*B*) High-K^+-induced Ca^{2+} influx was significantly inhibited by a mixture of voltage-sensitive Ca^{2+} channel blockers (*VSCCsX*). (*C*) Treatment with 50% D_2O BSS had no effect on the high-K^+-induced Ca^{2+} influx. (*D*) 90% D_2O BSS inhibited the high-K^+-induced Ca^{2+} influx only during D_2O washout. (*E*) Only 1 min treatment with 90% D_2O BSS was sufficient to inhibit several subsequent high-K^+-induced Ca^{2+} responses triggered during D_2O washout. (*F*) Longer treatment with 90% D_2O BSS (up to 17 min) did not significantly inhibit the high-K^+-induced Ca^{2+} influx triggered during treatment, but did result in a prolonged washout period during which high-K^+-induced Ca^{2+} influx was inhibited. The time course of changes in intracellular Ca^{2+} concentrations from four individual cells was plotted in all frames.

Ca^{2+} responses during D_2O washout (~9-min period; Fig. 5 *E*), whereas longer treatment (up to 17 min) with 90% D_2O BSS did not significantly affect high-K^+-induced Ca^{2+} influx induced during the treatment, but did lengthen the time course of high-K^+-induced Ca^{2+} influx (Fig. 5 *F*).

Effects of D_2O on voltage-dependent Ca^{2+} currents

To estimate kinetics of VSCCs during and after 90% D_2O exposure, we examined voltage-clamp recordings of Ba^{2+} currents in AtT20 cells. Although the gating kinetics of VSCCs for Ba^{2+} ions seems to be slightly modified during the D_2O exposure (Fig. 6 *A*), the maximal amplitude of Ba^{2+} currents activated by depolarizing voltage pulses was not significantly modified during and after 90% D_2O exposure. The reduction in the peak amplitude (−33.6 ± 19.9%) was observed during 90% D_2O treatment, but this difference was not statistically significant (Fig. 6 *A*; $n = 7$, n.s. by one way ANOVA).

The net Ca^{2+} currents were also analyzed by the voltage-clamp method. In this analysis, D_2O was applied by the bath perfusion as above, or by the patch pipette filled with 90% D_2O internal solution. The peak Ca^{2+} current recorded by the patch pipette filled with normal H_2O internal solution (−61.3 ± 19.0 pA at holding membrane potential of +10 mV, $n = 4$, Fig. 6 *B*) was not significantly modified by the perfusion of 90% D_2O BSS (−56.9 ± 4.0 pA, $n = 4$, data not shown). On the other hand, the Ca^{2+} currents recorded with the patch pipette filled with 90% D_2O internal solution were significantly smaller at positive holding membrane potentials (−15.4 ± 5.2 pA at holding membrane potential of +10 mV, $n = 8$, $p < 0.05$; Fig. 6 *B*). The current-voltage relationship of Ca^{2+} currents returned normally after additional 90% D_2O treatment by the bath perfusion (−55.1 ± 20.3 pA at holding membrane potential of +10 mV, $n = 8$; Fig. 6 *B*).

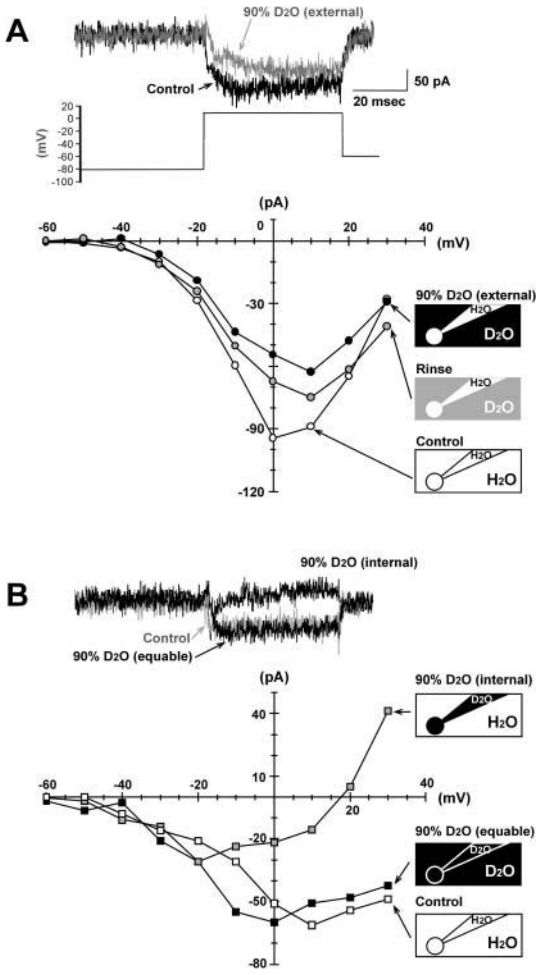

FIGURE 6 The effects of D_2O on voltage-sensitive Ca^{2+} channels were studied by voltage-clamp recordings of Ba^{2+} and Ca^{2+} currents. (*A*) The current-voltage curves for Ba^{2+} currents (average of seven cells) showing the little effects of 90% D_2O on the Ba^{2+} current amplitude over a range of depolarizing voltage steps. Example of Ba^{2+} currents activated by depolarizing voltage steps applied before and during bath perfusion with 90% D_2O is shown on the top. These Ba^{2+} currents were recorded by the whole-cell patch clamp method with internal solution of H_2O. (*B*) The current-voltage curves for Ca^{2+} currents (average of 3–8 cells) showing the significant modulation of current-voltage relationship when Ca^{2+} currents were recorded with internal solution of 90% D_2O. Note that inward currents at positive holding membrane potentials were significantly reduced with this recording condition. The current-voltage relationship of Ca^{2+} currents was recovered by the additional bath perfusion of 90% D_2O-BSS. Example of Ca^{2+} currents is shown on the top as above in *A*.

Effects of D_2O on β-endorphin release

Treatment with 90% D_2O BSS increased the release of β-endorphin slightly (126.6 ± 20.6% of H_2O control), but not to a statistically significant degree ($p = 0.11$; Fig. 7). Exposure to 30 mM K^+ resulted in a significantly greater release of β-endorphin compared with baseline levels both in H_2O BSS (138.0 ± 8.6% of H_2O control, $n = 5$, $p < 0.05$) and 90% D_2O BSS (163.0 ± 24.3% of D_2O control, $n = 6$, $p < 0.05$). The high-K^+-induced β-endorphin release was

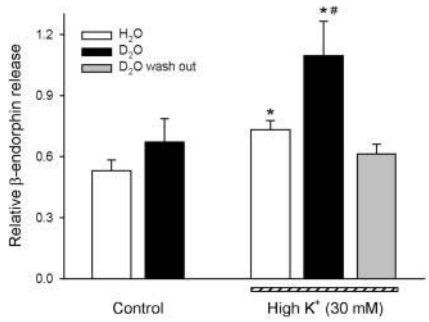

FIGURE 7 Effects of D_2O on β-endorphin release from AtT20 cells. β-Endorphin release was increased in 90% D_2O BSS compared to H_2O BSS. Exposure to 30 mM K^+ increased β-endorphin release in both H_2O and 90% D_2O BSS. Treatment with 90% D_2O BBS for 3 min inhibited the high-K^+-induced increase in β-endorphin release, not during the treatment itself but during the D_2O washout. The concentration of β-endorphin released overnight (16 h) under control conditions in each flask was used to normalize the variations among flasks. $^*p < 0.05$ by Student's *t*-test in comparison with corresponding control groups. Among three high-K^+-treated groups, concentration of β-endorphin was significantly higher in D_2O than other two groups ($F_{2,13} = 4.86$, $^{\#}p < 0.05$ by Duncan's multiple range test after one way ANOVA).

inhibited during washout of 90% D_2O BSS (115.6 ± 9.2% of H_2O control, $n = 5$, $p > 0.05$).

Theoretical estimation of the effects of D_2O treatment

Substitution of deuterium for hydrogen causes a number of observable effects of various kinds. These effects are generally understood in terms of the effect of mass on vibrational energy levels. We carried out quantum chemical calculations using the density functional theory. In the first step, we estimated the zero-point vibrational energy difference (ΔZPVE) for hydrophilic amino acids (Table 1). Within the hydrophilic amino acids, acidic amino acids were not analyzed in this simulation because they have only tight CH bounds at their side chains.

Here we assume simple exchange reactions:

(A·A)–OH + D_2O → (A·A)–OD + DOH (for Ser, Thr, and Tyr)

(A·A)–NH + D_2O → (A·A)–ND + DOH (for Asn, Gln, Lys, Arg, and His).

These data show that a single deuterium substitution lowered the zero-point vibrational energy by 2.10 ± 0.02 kcal/mol and a dual deuterium substitution doubled the ΔZPVE for several amino acids examined. Compared to a bond to hydrogen, a deuterium-containing bond has lower zero point energy. The activation energy is greater and the rate of the reaction is correspondingly less for the deuterated compounds. Within the Born-Oppenheimer approximation, deuterated and nondeuterated molecules are electronically identical, thus isotope effects arise primarily from the

ΔZPVE. These data indicate that for hydrophilic amino acids examined, the isotopic substitution of hydrogen by deuterium may be preferred over that of deuterium by hydrogen, which may result in slower deuterium to hydrogen exchange in these amino acids.

DISCUSSION

This study examined the effects of D_2O treatment on the physiological processes underlying β-endorphin release from AtT20 cells, and demonstrated several clear changes due to exposure to D_2O. First, changes that were observed during the actual treatment with D_2O were i), dynamic redistribution of actin filaments, ii), defilamentation of actin filaments, iii), partial inhibition of voltage-activated Na^+ and K^+ currents, iv), inhibition of spontaneous action potentials and Ca^{2+} oscillations, and v), increased high-K^+-induced β-endorphin release. During D_2O treatment, no changes were observed in i), the distribution of β-tubulin, ii), high-K^+-induced Ca^{2+} flux, and iii), high-K^+-induced membrane depolarization. Therefore, the most probable mechanism to enhance β-endorphin release within parameters analyzed here is a dynamic change in actin filaments. Second, more specific effects of D_2O were observed soon after D_2O treatment, during the washout of D_2O BSS, and the return to H_2O BSS. These changes were i), complete inhibition of high-K^+-induced Ca^{2+} flux, and ii), inhibition of high-K^+-induced β-endorphin release. This delayed effect of D_2O cannot be explained by solvent isotope effects, and thus it is reasonable to consider the purely isotope exchange effects in VSCCs and/or their regulatory proteins.

Cellular responses under D_2O exposure

Although classical interpretations of D_2O-induced inhibition of cellular secretion have been based on D_2O-mediated stabilization of microtubules (Malaisse-Lagae et al., 1971; Montague et al., 1976; Hill and Rhoten, 1983), the effects of D_2O on the cytoskeleton appear to be even more prevalent and varied. Zimmermann et al. (1988) reported that D_2O induces the redistribution of filamentous actin and a change in morphology of human neutrophil granulocytes. More recently, Omori et al. (1997) examined the effects of D_2O on actin filaments using fluorescent staining of BALB 3T3 cells and observed a transient increase in actin filaments. In addition, they examined the effects of D_2O on actin polymerization in vitro and demonstrated that D_2O accelerates purified globular actin polymerization immediately upon exposure to D_2O, whereas the total amount of polymerized actin later during treatment with D_2O is the same as that in H_2O. Therefore, one possible mechanism underlying D_2O-induced actin filament redistribution may involve the hydrogen to deuterium exchange in globular proteins (Hermans and Scheraga, 1959; Scheraga, 1960), which results in more stable protein structures (Sing and Wood, 1969; Karasz and Gajnos, 1976), and thus is caused by a typical isotope exchange effect.

The results of this study indicate that among several cytoskeletal components, D_2O affected actin filaments specifically. The effect of D_2O on the amount of actin filaments was transient (<15 min), which is consistent with Omori et al. (1997). Although we cannot exclude the possible action of D_2O on microfilaments with a longer application of D_2O, the results of our study indicate that it is possible to affect actin filaments selectively with our experimental protocol in AtT20 cells. In addition, we found a decrease in actin filaments in the cell processes immediately upon exposure to D_2O in AtT20 cells. Secretory vesicles are transferred to the cell processes for exocytosis in AtT20 cells (Tooze and Burke, 1987). The disassembly of the actin barrier at the plasma membrane is thought to be essential for the fusion of secretory vesicles (Pfeiffer et al., 1985; Koffer et al., 1990; Lejen et al., 2001; Wilson et al., 2001); therefore, D_2O-induced disassembly of the actin barrier may be the one possible mechanism to facilitate vesicle fusion, and β-endorphin release. Therefore, D_2O-induced increases in secretion observed in this study and in various other cell types (Bennett et al., 1979; Sulowska and Wyczolkowska, 1991; Fewtrell and Metzger, 1980; Maeyama et al., 1986; Urata et al., 1989) may be explained in part by actin-mediated mechanisms.

The D_2O-induced reduction in spontaneous action potentials and slight hyperpolarization of the resting potential both rapidly returned to control values upon D_2O washout. The direct action of D_2O on Na^+ channel gating has been demonstrated previously in *Myxicola* giant axons (Schauf and Bullock, 1979; Schauf and Chuman, 1986). Consistently, our study also demonstrated slow activation and inactivation of Na^+ channel kinetics during D_2O exposure in AtT20 cells. Since Na^+ channel activity is directly modulated by actin polymerization (Mironov and Richter, 1999; Negulyaev et al., 2000), it is also possible that D_2O indirectly effects on Na^+ channels via actin filaments. In addition, a reduction in the mobility of Na^+ in D_2O buffer is known as the solvent isotope effects (Bass and Moore, 1973). Therefore, both isotope exchange effects and solvent isotope effects may mediate the D_2O effects on spontaneous action potentials.

During D_2O exposure, we also found partial and reversible inhibition of spontaneous Ca^{2+} oscillations in AtT20 cells. Application of TTX did not inhibit spontaneous Ca^{2+} oscillations, indicating that these Ca^{2+} oscillations were not caused by voltage-dependent mechanisms. Since spontaneous Ca^{2+} oscillations were activated by caffeine and inhibited by dantrolene, the Ca^{2+} oscillations appears to be dependent on Ca^{2+} release from ryanodine-sensitive internal Ca^{2+} stores in AtT20 cells. D_2O inhibited both spontaneous and caffeine-activated Ca^{2+} oscillations, whereas neither high-K^+-induced Ca^{2+} influx nor voltage-dependent Ca^{2+} currents were affected during D_2O exposure. Therefore, D_2O

may affect proteins regulating Ca^{2+} release from internal stores, although the specific sequence for the inhibition of spontaneous Ca^{2+} oscillations still needs to be analyzed.

In the presence of high-K^+, exposure to D_2O increased β-endorphin release, whereas the D_2O-induced enhancement of β-endorphin release was not significant without high-K^+ stimulation. Considering observed D_2O actions on physiological processes underlying β-endorphin secretion, two interpretations are possible: i), the modulation of actin filaments alone is not sufficient to increase β-endorphin release, or ii), the inhibition of spontaneous action potentials and Ca^{2+} oscillations during D_2O treatment masked a concomitant D_2O-induced, actin-mediated increase in β-endorphin release. However, the identification of primary D_2O action for secretory activities during D_2O exposure is difficult in living cells, since various solvent isotope effects and isotope exchange effects are simultaneously produced during D_2O exposure and many of these effects are interrelated.

Cellular responses during D_2O washout

During D_2O washout, the high-K^+-induced Ca^{2+} influx was completely inhibited for several minutes and gradually recovered (Fig. 5). In contrast, the high-K^+-induced membrane depolarization of the membrane potential was not significantly affected during or after D_2O exposure and agreed well with that predicted by the Nernst equation for K^+ (Fig. 4 *A*). Although K^+ channel conductance estimated by the voltage-clamp recordings was partially reduced upon D_2O exposure, no further reductions in K^+ currents were observed upon D_2O washout (Fig. 4 *C*). Therefore, complete inhibition of the high-K^+-induced Ca^{2+} influx upon D_2O washout appears to involve VSCCs themselves and not via the effects on K^+ channels. Because secretion from AtT20 cells depends on Ca^{2+} dynamics that are regulated largely by VSCCs in AtT20 cells (Richardson and Schonbrunn, 1981; Richardson, 1983), it is reasonable to assume that the inhibition of high-K^+-induced β-endorphin release may be associated with the reduction of the high-K^+-induced Ca^{2+} influx.

To further clarify the effects of D_2O on VSCCs, we examined Ba^{2+} and Ca^{2+} current recordings by the voltage clamp electrophysiology. Interestingly, with the conventional whole-cell patch-clamp recordings with an electrode pipette filled with H_2O internal solution, we could not observe any significant reductions in the current amplitudes during or after D_2O exposure (Fig. 6 *A*). However, when the D_2O was dialyzed into the cells by the patch electrode, the current-voltage relationship of Ca^{2+} currents was modulated with a significant decrease in the inward currents (Fig. 6 *B*). The results suggest that asymmetric distribution of D_2O (intracellular) and H_2O (extracellular) across the plasma membrane is critical for the inhibition of VSCCs. Since intracellular D_2O concentration in intact cells is higher than the extracellular D_2O concentration during D_2O washout, the inhibition of high-K^+-induced Ca^{2+} influx may be explained by the asymmetric distribution of D_2O that was produced exclusively during D_2O washout.

Andjus et al. (1994) reported that asymmetric distribution of D_2O (extracellular) and H_2O (intracellular) across the plasma membrane of freshwater alga activated Ca^{2+} channels in these cells. This effect of D_2O may involve direct activation of Ca^{2+} channels, because the open channel probability of Ca^{2+} channels reconstituted in lipid bilayers is also increased in D_2O. The authors suggested that transient osmotic-like stress produced by the more rapid transmembrane diffusion of D_2O may mediate the activation of Ca^{2+} channels (Brooks, 1937). However, we could not find any cell shape changes during and after the D_2O exposure (Fig. 3), and thus the involvement of stress-sensitive mechanisms in the high-K^+-induced Ca^{2+} influx can be ruled out. In addition, solvent isotope effects cannot explain the delayed D_2O effects on high-K^+-induced Ca^{2+} influx. Therefore, replacement of hydrogen with deuterium in constitutive proteins of VSCCs or in their regulatory proteins asymmetrically across plasma membrane may be the most considerable mechanism for the modulation of VSCCs.

Despite the significant inhibition of high-K^+-induced Ca^{2+} influx during D_2O washout, the same was not observed when the cells were treated in the presence of 90% D_2O BSS, even with long incubation periods (up to 17 min), suggesting that the inhibition of Ca^{2+} flux was not associated with the onset of exposure to D_2O or the duration of D_2O treatment but with the return to H_2O. Consistently, Ca^{2+} currents recorded with equable D_2O substitutions in intracellular and extracellular solutions displayed normal current-voltage relationship (Fig. 6 *B*). These results suggest that the Ca^{2+} conductance of VSCCs is greatly affected in the intermediate state of isotope exchange effects when the constitutive proteins of VSCCs or their regulatory proteins contain asymmetrically deuterated amino acids during D_2O washout, but not in the steady state when amino acids are completely deuterated during D_2O treatment in the constitutive proteins of VSCCs or in their regulatory proteins (models in Fig. 8).

The intermediate state of isotope exchange effects is explained by a difference in the stability of proteins; deuterated proteins are more stable than protonated proteins (Omori et al., 1997; Chakrabarti et al., 1999). Of the many known effects due to the differences in reactivity of deuterium bonds versus hydrogen bonds, the one most relevant to the effects observed in this study may be the zero-point energy differences. Our quantum chemical calculations indicate that the isotopic substitution of hydrogen by deuterium lowers the total energy of hydrophilic amino acids because of the decrease in zero-point vibrational energy (Table 1). Therefore, it is likely that cells rapidly reach equilibrium after an exchange of H_2O for D_2O, but take a longer time to reach equilibrium after switching from D_2O back to H_2O in these proteins. Within the hydrophilic

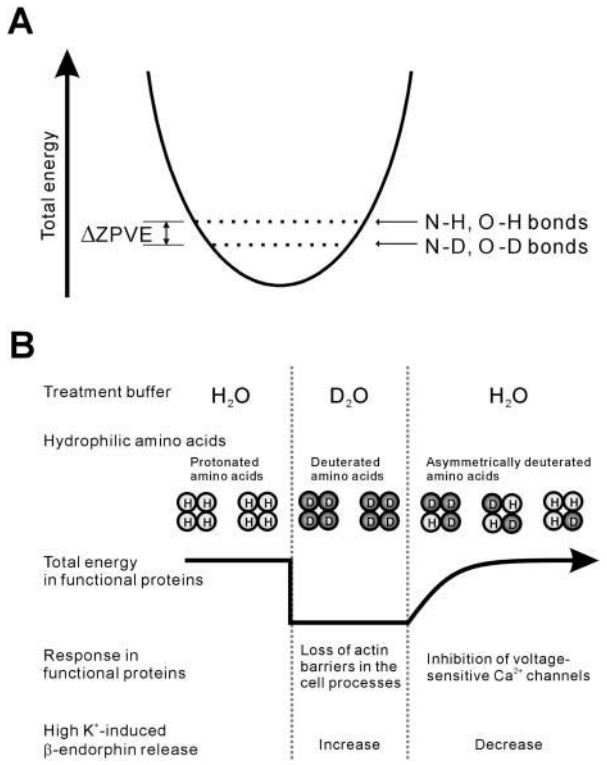

FIGURE 8 (*A*) Schematic illustration of changes in the zero-point vibrational energy when hydrogen is exchanged for deuterium in hydrophilic amino acid residues of proteins. Solid curve denotes the electronic energy of the system. Single deuterium substitution for hydrogen reduces the binding energy ~2.1 kcal/mol ($\Delta ZPVE$) in hydrophilic amino acids. The total reduction of vibrational energy reduction in functional proteins depends on the number of deuterated amino acids replaced. (*B*) For the energy differences between protonated and deuterated amino acids, the replacement of H_2O buffer with D_2O buffer immediately converts protonated amino acids to deuterated amino acids, whereas deuterated amino acids slowly convert to protonated amino acids after replacement of D_2O buffer with H_2O buffer. The difference of exchange rates produces long-lasting transient states with asymmetrically deuterated amino acids. The increase in the high-K^+-induced β-endorphin release is in phase with the deuterated amino acids, and the most probable cause is due to the loss of actin filament barriers in the cell processes, although this effect coincides with many other effects including solvent isotope effects. The decrease in the high-K^+-induced β-endorphin release is in phase with asymmetrically deuterated amino acids, and the most probable cause is the inhibition of voltage-sensitive Ca^{2+} channels.

amino acids, a relatively large ΔZPVE was found in tyrosine that is known as a critical residue for the voltage sensor of L-type Ca^{2+} channels (Bodi et al., 1997). Thus, this may produce a relatively long-lasting transient state in VSCCs with asymmetric deuterated amino acids after treatment of D_2O buffer that will inhibit the activity of VSCCs.

There are many known sites and mechanisms of action for D_2O on cellular secretion. Both D_2O-induced inhibition and activation of secretion have been reported in many different cell types. The results of this study demonstrated biphasic and bidirectional effects of D_2O on β-endorphin release that may be linked to the effects of D_2O on actin filaments and VSCCs. Since the D_2O concentration is only 1/6700 of H_2O in our environment, hydrogen/deuterium exchange effects on natural living systems may be negligible. However, the results answered the complex D_2O actions on cellular secretions in experimental models that were controversial for decades.

This work was supported in part by a grant for Research for the Future Program (96L00310 to T.Y.) from Japan Society for the Promotion of Science, a grants-in-aid for scientific research (B14380372) by the Ministry of Education, Culture, Sports, Science and Technology, Japan to M.I., and a grant from the National Institutes of Health (NS036607) to C.N.A.

REFERENCES

Andjus, P. R., A. A. Kataev, A. A. Alexandrov, D. Vucelic, and G. N. Berestovsky. 1994. D_2O-induced ion channel activation in Characeae at low ionic strength. *J. Membr. Biol.* 142:43–53.

Bass, L., and W. J. Moore. 1973. The role of protons in nerve conduction. *In* Progress in Biophysics and Molecular Biology. Vol. 27. A. J. V. Butler and D. Noble, editors. Pergamon Press, Oxford and New York. 143–171

Becke, A. D. 1993. Density-functional thermochemistry. III. The role of exact exchange. *J. Chem. Phys.* 98:5648–5652.

Bennett, W. F., J. S. Belville, and G. Lynch. 1979. A study of protein phosphorylation in shape change and Ca^{2+} dependent serotonin release by blood platelets. *Cell.* 18:1015–1023.

Bodi, I., H. Yamaguchi, M. Hara, M. He, A. Schwartz, and G. Varadi. 1997. Molecular studies on the voltage dependence of dihydropyridine action on L-type Ca^{2+} channels. *J. Biol. Chem.* 272:24952–24960.

Brooks, S. C. 1937. Osmotic effects of deuterium oxide (heavy water) on living cells. *Science.* 86:497–498.

Calderon, P., J. Furnelle, and J. Christophe. 1980. Phosphatidylinositol turnover and calcium movement in the rat pancreas. *Am. J. Physiol.* 238:G247–G254.

Chakrabarti, G., S. Kim, M. L. Gupta, Jr., J. S. Barton, and R. H. Himes. 1999. Stabilization of tubulin by deuterium oxide. *Biochemistry.* 38:3067–3072.

Fewtrell, C., and H. Metzger. 1980. Larger oligomers of IgE are more effective than dimers in stimulating rat basophilic leukemia cells. *J. Immunol.* 125:701–710.

Freinkel, N., C. E. Younsi, and R. M. C. Dawson. 1976. Insulin release and phosphate ion efflux from rat pancreatic islets induced by L-leucine and its nonmetabolizable analogue, 2-aminobicyclo[2.2.1]heptane-2-carboxylic acid. *Proc. Natl. Acad. Sci. USA.* 73:3403–3407.

Frisch, M. J., G. W. Trucks, H. B. Schlegel, G. E. Scuseria, M. A. Robb, J. R. Cheeseman, V. G. Zakrzewski, J. A. Montgomery, Jr., R. E. Stratmann, J. C. Burant, S. Dapprich, J. M. Millam, A. D. Daniels, K. N. Kudin, M. C. Strain, O. Farkas, J. Tomasi, V. Barone, M. Cossi, R. Cammi, B. Mennucci, C. Pomelli, C. Adamo, S. Clifford, J. Ochterski, G. A. Petersson, P. Y. Ayala, Q. Cui, K. Morokuma, D. K. Malick, A. D. Rabuck, K. Raghavachari, J. B. Foresman, J. Cioslowski, J. V. Ortiz, A. G. Baboul, B. B. Stefanov, G. Liu, A. Liashenko, P. Piskorz, I. Komaromi, R. Gomperts, R. L. Martin, D. J. Fox, T. Keith, M. A. Al-Laham, C. Y. Peng, A. Nanayakkara, M. Challacombe, P. M. W. Gill, B. Johnson, W. Chen, M. W. Wong, J. L. Andres, C. Gonzalez, M. Head-Gordon, E. S. Replogle, and J. A. Pople. 1998. Gaussian 98, Reversion A.9. Gaussian, Inc., Pittsburgh, PA.

Furui, T., K. Satoh, Y. Asano, S. Shimosawa, M. Hasuo, and T. L. Yaksh. 1984. Increase of β-endorphin levels in cerebrospinal fluid but not in plasma in patients with cerebral infarction. *J. Neurosurg.* 61:748–751.

Harty, R. F., P. A. Franklin, and J. E. McGuigan. 1983. Effect of deuterium oxide on gastrin release from rat antral mucosal fragment. *Regul. Pept.* 7:171–181.

Hermans, J. Jr., and H. A. Scheraga. 1959. The thermally induced configurational change of ribonuclease in H_2O and D_2O. *Biochim. Biophys. Acta.* 36:534–535.

Hill, R. S., and W. B. Rhoten. 1983. Differential effects of microtubule-altering agents on beta-cells during development. *Am. J. Physiol.* 245: E391–E400.

Hirono, M., K. Takamura, Y. Ito, Y. Nakano, Y. Chikaoka, N. Suzuki, and T. Yoshioka. 1999. Role of Ca^{2+}-ATPase in spontaneous oscillation of cytosolic free Ca^{2+} in GH3 rat pituitary cells. *Cell Calcium.* 25:125–135.

Houston, L. L., J. Odell, Y. C. Lee, and R. H. Himes. 1974. Solvent isotope effects on microtubule polymerization and depolymerization. *J. Mol. Biol.* 87:141–146.

Ikeda, M., C. S. Nelson, H. Shinagawa, T. Shinoe, T. Sugiyama, C. N. Allen, D. K. Grandy, and T. Yoshioka. 2001. Cyclic AMP regulates the calcium transients released from IP_3-sensitive stores by activation of rat κ-opioid receptors expressed in CHO cells. *Cell Calcium.* 29:39–48.

Itoh, T. J., and H. Sato. 1984. The effects of deuterium oxide (^2H_2O) on the polymerization of tubulin in vitro. *Biochim. Biophys. Acta.* 800:21–27.

Karasz, F. E., and G. E. Gajnos. 1976. Relative stability of the α-helix of deuterated poly(γ-benzyl-L-glutamate). *Biopolymers.* 15:1939–1950.

Koffer, A., P. E. R. Tatham, and B. D. Gomperts. 1990. Changes in the state of actin-during the excocytotic reaction of permeabilised rat mast cells. *J. Cell Biol.* 111:919–927.

Kohn, W., and L. J. Sham. 1965. Self-consistent equations including exchange and correlation effects. *Phys. Rev.* 140:A1133–A1138.

Kushner, D. J., A. Baker, and T. G. Dunstall. 1999. Pharmacological uses and perspectives of heavy water and denatured compounds. *Can. J. Physiol. Pharmacol.* 77:79–88.

Lacy, P. E., S. L. Howell, D. A. Young, and C. J. Fink. 1968. New hypothesis of insulin secretion. *Nature.* 219:1177–1179.

Lee, C., W. Yang, and R. G. Parr. 1988. Development of the Colle-Salvetti correlation-energy formula into a functional of the electronic density. *Phys. Rev.* B37:785–789.

Lejen, T., K. Skolnik, S. D. Rose, M. G. Marcu, A. Elzagallaai, and J. M. Trifaro. 2001. An antisense oligodeoxynucleotide targeted to chromaffin cell scinderin gene decreased scinderin levels and inhibited depolarization-induced cortical F-actin disassembly and exocytosis. *J. Neurochem.* 76:768–777.

Loechner, K. J., R. M. Kream, and K. Dunlap. 1996. Calcium currents in a pituitary cell line (AtT-20): differential roles in stimulus-secretion coupling. *Endocrinology.* 137:1429–1437.

Maeyama, K., R. J. Hohman, H. Metzger, and M. A. Beaven. 1986. Quantitative relationships between aggregation of IgE receptors, generation of intracellular signals, and histamine secretion in rat basophilic leukemia (2H3) cells. Enhanced responses with heavy water. *J. Biol. Chem.* 261:2583–2592.

Malaisse, W. J., F. Malaisse-Lagae, E. V. Obberghen, G. Somers, G. Devis, M. Ravazzola, and L. Orci. 1975. Role of microtubule in the phasic pattern of insulin release. *Ann. N. Y. Acad. Sci.* 253:630–652.

Malaisse-Lagae, F., M. H. Greider, W. J. Malaisse, and P. E. Lacy. 1971. The stimulus-secretion coupling of glucose-induced insulin release. IV. The effect of vincristine and deuterium oxide on the microtubular system of the pancreatic B-cells. *J. Cell Biol.* 49:530–535.

Mironov, S. L., and D. W. Richter. 1999. Cytoskeleton mediates inhibition of fast Na^+ current in respiratory brainstem neurons during hypoxia. *Eur. J. Neurosci.* 11:1831–1834.

Montague, W., S. L. Howell, and I. C. Green. 1976. Insulin release and microtubular system of the islets of Langerhans: effects of insulin secretagogues on microtubule subunit pool size. *Horm. Metab. Res.* 8:166–169.

Negulyaev, Y. A., S. Y. Khaitlina, H. Hinssen, E. V. Shumilina, and E. A. Vedernikova. 2000. Na^+ channel activity in leukemia cells is directly controlled by actin polymerization. *J. Biol. Chem.* 275:40933–40937.

Nelson, C. S., M. Ikeda, H. S. Gompf, M. L. Robinson, N. K. Fuchs, T. Yoshioka, K. A. Neve, and C. N. Allen. 2001. Regulation of melatonin 1a receptor signaling and trafficking by asparagine-124. *Mol. Endocrinol.* 15:1306–1317.

Omori, H., M. Kuroda, H. Naora, H. Takeda, Y. Nio, H. Otani, and K. Tamura. 1997. Deuterium oxide (heavy water) accelerates actin assembly in vitro and changes microfilament distribution in cultured cells. *Eur. J. Cell Biol.* 74:273–280.

Pfeiffer, J. R., J. C. Seagrave, B. H. Davis, G. G. Deanin, and J. M. Oliver. 1985. Membrane and cytoskeletal changes associated with IgE-mediated serotonin release from rat basophilic leukemia cells. *J. Cell Biol.* 101:2145–2155.

Richardson, U. I. 1983. Adrenocorticotropin secretion by mouse pituitary tumor cells in culture: the role of Ca^{2+} in stimulated and somatostatin-inhibited secretion. *Endocrinology.* 113:62–68.

Richardson, U. I., and A. Schonbrunn. 1981. Inhibition of adrenocorticotropin secretion by somatostatin in pituitary cells in culture. *Endocrinology.* 108:281–290.

Sasaki, S., and Y. Tashiro. 1976. Studies on the posterior silk gland of the silkworm *Bombyx mori*. VI. Distribution of microtubule in posterior silk gland cells. *J. Cell Biol.* 71:565–574.

Schauf, C. L., and J. O. Bullock. 1979. Modification of sodium channel gating in Myxicola giant axons by deuterium oxide, temperature, and internal cations. *Biophys. J.* 27:193–208.

Schauf, C. L., and M. A. Chuman. 1986. Mechanism of sodium channel gating revealed by solvent substitution. *In* Neural Membranes. Alan R. Liss, Inc., New York. 3–23.

Scheraga, H. A. 1960. Helix-coil transformation in deuterated macromolecules. *Ann. N. Y. Acad. Sci.* 16:608–616.

Schetcterson, L. C., and G. S. McKnight. 1991. Role of cyclic adenosine 3′,5′-monophosphate-dependent protein kinase in hormone-stimulated beta-endorphin secretion in AtT20 cells. *Mol. Endocrinol.* 5:170–178.

Sing, T. R., and J. L. Wood. 1969. Isotope effect on the hydrogen bound length. *J. Chem. Phys.* 50:3572–3576.

Sulowska, Z., and J. Wyczolkowska. 1991. 5-Hydroxytriptamine releasing activity of supernatants from cultured mouse spleen cells. *Arch. Immunol. Ther. Exp. (Warsz.).* 39:139–145.

Suzuki, N., M. Hirono, K. Kawahara, and T. Yoshioka. 1997a. Sapecin B, a novel fly toxin, blocks macroscopic K^+ currents in the GH3 rat pituitary cell line. *Am. J. Physiol.* 273:C289–C296.

Suzuki, N., M. Hirono, H. Takagi, and T. Yoshioka. 1997b. Facilitation of Ca^{2+} action potential frequency by a small G protein Rab3A in rat pituitary GH3 cells. *Biochem. Biophys. Res. Commun.* 235:331–335.

Tooze, J., and B. Burke. 1987. Accumulation of adrenocorticotropin secretory granules in the midbody of telophase AtT20 cells: evidence that secretory granules move anterogradely along microtubules. *J. Cell Biol.* 104:1047–1057.

Urata, C., A. Watanabe, Y. Ogawa, N. Takei, H. Nomoto, M. Mizobe, Y. Abe, K. Mano, and S. Urata. 1989. Effect of deuterium oxide (D_2O) on the IgE-mediated Ca^{2+} influx, arachidonic acid and histamine release in rat basophilic leukemia. *Arerugi.* 38:285–295.

Westendorf, J. M., and A. Schonbrunn. 1985. Peptide specificity for stimulation of corticotropin secretion: activation of overlapping pathways by the vasoactive intestinal peptide family and corticotropin-releasing factor. *Endocrinology.* 116:2528–2535.

Wilson, J. R., R. I. Ludowyke, and T. J. Biden. 2001. A redistribution of actin and myosin IIA accompanies Ca^{2+}-dependent insulin secretion. *FEBS Lett.* 492:101–106.

Zimmermann, A., H. U. Keller, and H. Cottier. 1988. Heavy water (D_2O)-induced shape changes, movements and F-actin redistribution in human neutrophil granulocytes. *Eur. J. Cell Biol.* 47:320–326.